Microcrystalline Cellulose from Aloe Plant Waste as a Platform for Green Materials: Preparation, Chemical Functionalization, and Application in 3D Printing

Microcrystalline cellulose from Aloe plant waste as platform for green materials: preparation, chemical functionalization and application in 3D printing

Maria Chiara Cabua,[a] Maria Vittoria Piras,[a] Debora Dessi,[b] Giorgia Sarais,[b] Francesco Corrias,[b] Michael Zanon,[c] Keivan Guido Kahnamoei,[a] Alberto Martis,[c] Guido Ennas,[a] Ignazio Roppolo,[d] Candido Fabrizio Pirri,[c,d] Alessandra Cabizza,[e] Annalisa Chiappone,[a] Francesco Secci,[a]*

[a] Dipartimento di Scienze Chimiche e Geologiche, Università degli Studi di Cagliari, Complesso Universitario di Monserrato, 09042, Monserrato (Cagliari), Italy
[b] Dipartimento di Scienze della Vita e dell'Ambiente, Università degli Studi di Cagliari, Complesso Universitario di Monserrato, 09042, Monserrato (Cagliari), Italy
[c] Center for Sustainable Future Technologies (CSFT)@Polito, Istituto Italiano di Tecnologia, Via Livorno 60, Torino, 10144, Italy
[d] Dipartimento di Scienza Applicata e Tecnologia, Politecnico di Torino, C.so Duca degli Abruzzi 24, 10129 Turin, Italy
[e] Lab7 Srl, Via San Tommaso D'Aquino 18/a, 09134 Cagliari

Corresponding author: Francesco Secci, fsecci@unica.it

Abstract

Aloe represents a valuable resource for the Mediterranean economy, pharmaceutical and nutraceutical industries exploit the Aloe gel for several applications but about 45wt% of the Aloe plant, i.e. the leaf peel, is waste. This waste is usually disposed of in a landfill or used as fertilizer. The possibility to give added value and a second life to the portions of Aloe Vera waste will help this growing market enter a circular economy perspective.

In this work, waste collected from local Sardinian cultivation of Aloe Vera was employed to prepare microcrystalline cellulose (MCC). Cellulose was purified from anthraquinones, lignin, and hemicellulose through hydrolytic procedures using eco-friendly solvents. Anthraquinone biocomponents were quantified as well as lignin and hemicellulose and intended for other valorization processes. At the same time, the cellulose fraction was further converted into MCC and characterized by NMR and infrared spectroscopy, and X-ray analyses. TGA-IR and SEM microscopy analyses were performed to investigate the structural changes of MCC during the extraction and post-functionalization processes. MCC derivatives were finally used as crosslinkers in the photopolymerization and light-induced 3D printing (VAT printing) of acrylic monomers and hydrogels.

Keywords: Agrifood waste; Aloe; cellulose; VAT polymerization; 3D printing

Introduction

With the increase of food and natural resources consumption, agricultural waste generation has grown considerably since the last century with a relevant environmental impact on the planet. [1,2] In this context, global efforts are devoted to obtain residual resources from waste and to apply them in various fields

spanning from energy production to high-tech applications.[3] Consequently, valorization of wastes generated from primary processing of crop raw materials is nowadays recognized as an opportunity for a technological development creating virtuous sustainable economies.[1] Recently, cellulose, lignin and lipid fractions from biomass have gained particular interest for the production of new generation bulk chemicals and fuels.[4,5] In this scenario, here we focus our efforts on obtaining materials with high technological value from Aloe Vera local waste. This plant, also called Barbadensis Miller, is cultivated in warm climatic areas of Asia, Europe and America and globally the hectares of soil dedicated to the A. Vera cultivation are estimated in ca. 25.000 (19.500 America, 300 Africa, 4.300 Australasia; 1200 Europe) with a world production of around 700 thousand tons per year and the market size of Aloe extracts is valued 2.6 USD billion in 2023 and is forecasted to grow of the 8% between 2024 and 2032.[6–9] However, during the industrial Aloe processing about the 45% of the starting material weight is discarded, generating large amounts of waste.[10] This huge biomass material has been proposed as bio-based adsorbent for the removal of water pollutants and heavy metals[11] for energy purposes[12] and as a supplement of lactating cows to improve milk production performances.[13] On the other hand, with the entry in force of Regulation (EU) 2021/468 of 18th of March (which amends Annex III of Regulation (EC) No. 1925/2006), the UE has banned Aloe-based supplements containing hydroxy anthracene, Aloe-emodin, emodin, dantron and its derivatives. This meant that the processing procedures of Aloe leaves and their transformation were monitored in such a way as to ensure batch uniformity and compliance with current legislation, leading to the production of additional waste and increasing the costs for the transformation companies. In this context, we decided to investigate other potential uses of Aloe Vera processing waste with particular attention to cellulosic materials extraction, with the aim to develop a bio-based platform that could enhance these industrial wastes.[1] Herein we report a study rooted on the extraction and purification of cellulose from the processing waste of South Sardinia grown Aloe and in particular we focused our attention in the preparation of a series of functionalized MCCs and their use as bio-fillers and crosslinkers for polymeric 3D printable formulations, showing how this waste can be turned in a substrate for several reactions and substituted to petroleum-based chemicals.

Materials and methods

Materials

The processing scraps of Aloe Vera leaves, grown in Southern Sardinia, were supplied by the company Lab7 (Cagliari, Italy). Aloe waste recovered from the processing plant in September 2022 was used. Commercial MCC used as comparison was purchased from Fisher Scientific. Sulfuric acid, hydrogen peroxide (30% v/v), sodium carbonate, hydrochloric acid (37%), sodium hydroxide, Methacrylic anhydride (MA, 94 %), phthalic anhydride, 4-bromo-benzoyl chloride, phthaloyl chloride and allylamine, Gelatin from cold-water Fish skin (powder, gelling point < 10 °C, CFG), Polyethylene glycol diacrylate Mw575 (PEGDA), Phenylbis(2,4,6-trimethylbenzoyl)phosphine oxide (BAPO),

lithium phenyl-2,4,6 trimethylbenzoylphosphinate (LAP), were purchased from Sigma Aldrich and used as received. Methanol, ethanol, dimethylacetamide, dimethylformamide were purchased from Carlo Erba and used as received.

Aloe waste treatment and MCC extraction

Biomass from Aloe waste was cut in small pieces (ca. 3x3 cm) and submitted to freeze-drying process. The collected dry peels were ball milled to afford sieved homogeneous powders with about 200μm diameter (Table S1). Samples of Aloe powders were then submitted to Soxhlet extraction using ethanol to remove the lipidic fraction, chlorophylls and the majority of anthraquinone species (AQs) as previously reported. [14] Subsequently, Aloe powders (~17g) were submitted to solvothermal hydrolysis to remove the lignocellulosic materials from cellulose. This process was performed in an autoclave (Teflon autoclave with a steel jacket, 300ml) using a 1:1 H_2O-EtOH mixture (90ml) in the presence of sulfuric acid (0.05 M) at 150°C for 6h.

After being brought back to room temperature, the solid was filtered and washed with hot distilled water. The filtered solid was then dried under vacuum at 50 °C. Subsequently, whitening of the cellulose was performed. Cellulose bleaching reactions were conducted as follows: Cellulose was suspended in a water solution of H_2O_2 (30% v/v), Na_2CO_3 (80mg/mL) at 60 °C under stirring for 10 hours (cellulose/solution ratio 1:10). Once cooled to room temperature, the solid was filtered under reduced pressure. The samples were then dried under vacuum at 50° C. The so obtained cellulose was suspended in a aqueous solution of HCl 37% and stirred at 80 °C for one hour to afford MCC as a pure product. This procedure allowed to obtain about 4.8g of material (yeld 28%) After that time, the suspension was neutralized by adding dropwise an aqueous solution of NaOH until pH 7 was reached. The resulting media was left to rest for 10 hours at room temperature to allow MCC precipitation. MCC was filtered and washed with ethanol and dried under vacuum at 60 °C for 10 hours.

MCC functionalization

A series of easy-to-introduce functional groups were selected and in particular the MCCs were reacted in separate experiments with: a) methacrylic anhydride), b) phthalic anhydride, c) phthaloyl chloride / allylamine and d) 4-bromobenzoyl chloride.

Preparation of MAcr-MCC using methacrylic anhydride: Dry MCC (1.0 g) was added to a hot dimethylacetamide (DMAc) solution at 80 °C (1% w/v). After 30 minutes, dry LiCl (8% w/v) was added, and the solution was stirred for 3 h at 80 °C under nitrogen atmosphere. Then, the temperature was reduced to 50 °C and the solution was kept stirring overnight, until complete dissolution. This solution was cooled down to room temperature and methacrylic anhydride (methacrylic anhydride/ glucose ring ratio = 10:1mol/mol) 9.66 mL (0.061 mol) and triethylamine (9.34 mL, 0.067 mol) were added. The resulting solution was stirred for 16 hours. The mixture was precipitated by adding ethanol

portionwise (10 mLx10) and the obtained white powder (1.026 g) was washed with ethanol several times and dried at room temperature under reduced pressure. [15] Glucose substitution calculated on the basis of the 13C CP/MAS analysis of MAcr-MCC: 0.33.

Preparation of PhtOH-MCC using phthalic anhydride: Phthalic anhydride (10 g, 0.067 mol) was stirred with dry Aloe Vera MCC (1.0 g), (phthalic anhydride/glucose ring ratio10:1 mol/mol), at 135 °C for 2 hours under neat conditions. Then, the mixture was cooled to RT and washed with acetone (2x100 mL) and distilled water (2x100 mL). The resulting solid (1.015 g) was separated by centrifugation and dried under reduced pressure as a crystalline white solid.[16] Glucose substitution calculated on the basis of the ^{13}C CP/MAS analysis of PhtOH-MCC: 0.017.

Preparation of PhtAm-MCC using a two-step phthaloyl chloride/allylamine reaction: Dry MCC (1.0 g) was added to a 80 °C DMAc (100 mL) stirred solution under nitrogen atmosphere. After 30 minutes, dry LiCl (0.8 g) was added and the resulting suspension was stirred for further 3 hours at the same temperature. After this time, the temperature was reduced to 50 °C and the solution was stirred overnight until complete dissolution. After this time the reaction mixture was cooled down to room temperature and in sequence, triethylamine (6.9 mL, 0.049 mol) and phthaloyl chloride (phthaloyl chloride/glucose ring 10:1 mol/mol) 7.1 mL (0.049 mol) were added dropwise.[17] The resulting solution was stirred for 16 h then allylamine (2.13 mL, 0.047 mol) was added dropwise. After 10 h reaction, ethanol (10 mLx10) was added portionwise to induce the precipitation of a brown powder. The resulting solid was washed with ethanol (2x100 mL), then the solvent was removed under reduced pressure at room temperature to afford 1.032 g of PhtAm-MCC as a pale yellow solid. Glucose substitution calculated on the basis of the ^{13}C CP/MAS analysis of PhtAm-MCC: 0.031.

Preparation of BBz-MCC using 4-bromo-benzoyl chloride: Dry MCC (1.0 g) was added to a hot DMAc solution at 80 °C (1% w:v). After 30 minutes, dry LiCl (8% w:v) was added and the solution was stirred for further 3 h at the same temperature under nitrogen atmosphere. Then, the temperature was reduced to 50 °C and the solution was kept stirring overnight, until complete dissolution. The solution was cooled down to room temperature and 4-bromo benzoyl chloride (4-bromo benzoyl chloride/glucose ring ratio 10:1 mol/mol) 10 g, (0.045 mol) and triethylamine (6.34 mL, 0.045 mol) were added dropwise. The resulting reaction mixture was stirred overnight. The reaction mixture was precipitated by the portionwise addition of ethanol (10 mLx10). The obtained light brown powder (1.24 g) was washed with ethanol several times (3x50 mL) and dried at room temperature under reduced pressure to afford 1.021 g of a beige solid. Glucose substitution calculated on the basis of the ^{13}C CP/MAS analysis of BBz-MCC: 0.028.

Preparation of the photocurable formulations and DLP printing

Methacrylated MCC (MAcr-MCC) was used as filler for the synthesis of gelatin-MCC based hydrogels. Methacrylated gelatine (GelMA) was produced as described elsewhere. [18] Dry GelMA was dissolved in

deionized water (15wt%), different amounts of MAcr-MCC were added to the water-based formulation (5, 10 wt%, with respect to the total amount), that was magnetically stirred for 2 hours. Afterward LAP (water-soluble photoinitiator) was added (2phr). The same samples were produced using neat MCC as a comparison. The prepared formulations are summarized in Table S2.

MAcr-MCC was also added to the commercial monomer polyethyleneglycol diacrylate (PEGDA) in different amounts, i.e. 5, 10, 20,33 wt%; neat MCC was also added to PEGDA. (Table S2): The cellulose powder was added to the liquid resin and magnetically stirred at room temperature for 2 hours, subsequently BAPO (2phr) was added.

GelMAcr-MCC 5 and PEGDA-MAcr-MCC 20 formulations were 3D-printed using an ASIGA UV-MAX X27 DLP printer (XY pixel resolution of 27 μm; diode source emitting at 385 nm). Different 3D models were designed, using Solidworks 2019 CAD software, converted in STL file formats and 3D-printed. The printing parameters are detailed in Table S3 for each formulation. Lastly, the printed objects were post-cured for 3 min under UV-light (12 mW/cm^2, medium- pressure mercury lamp provided by Robot Factory).

Characterization

Waste composition analyses

Van Soest method: The composition of the Aloe waste was analysed for cellulose, hemicellulose and lignin content using acid detergent fibre (ADF), neutral detergent fibre (NDF) and acid detergent lignin (ADL) methods, respectively according to standard procedure described by Van Soest et al. [19]In this method 1 g air dried waste powder was digested for 2 hour with 100 mL neutral detergent solution (sodium lauryl sulphate 30g, disodium ethylenediamine tetraacetatic acid 18.61 g/L, sodium borate 6.18 g/L, anhydrous disodium hydrogen phosphate 4.56 g/L, ethylene glycol monoethyl ether10 mL) to obtain the insoluble components of the original powder. The residue containing cellulose, hemicellulose and lignin was washed with boiled water followed by acetone, dried at 100 °C and weighed. The resulting sample was refluxed with 100 mL of an acid detergent solvent (H_2SO_4 49 g/L, cetyl trimethylammonium bromide 20 g/L) for 1 h aiming to solubilize the hemicellulose fraction. After filtration the residue was washed angain, dried at 100 °C and weighed. The last residue containing cellulose and lignin was treated with 72 % sulfuric acid for 3 h for the dissolution of cellulose, leaving lignin in the residue which was washed, dried at 100 °C and weighed. The ADF value refers to the portions of the cell wall composed of cellulose and lignin, while ADL indicates exclusively the lignin portion present in the sample. Therefore, the calculation of the cellulose value is performed as a subtraction of the ADF value from that of ADL, while for hemicellulose the NDF value is subtracted from that of ADF.

Ash analysis: The analysis of the ash was conducted according to the AOAC method (1990) Official Methods of Analysis: (15thedn), Association of Official Analytical Chemists, Washington, D.C. A porcelain crucible was washed and then heated in an oven to 100 °C, left to cool in a desiccator and then weighed on the analytical balance. Afterwards the Aloe peel powder was inserted into the crucible which was then placed in a muffle for 4 hours at a temperature of 600 °C. At the end, the crucible was cooled in a desiccator and weighed again.

Antraquinones quantification: An aliquot of the extracted solution, appropriately filtered, was injected into HPLC-DAD for the determination of the main anthraquinone compounds. The analysis was carried out in a binary gradient using the following solvents: H_3PO_4 0.22 M (A) and Acetonitrile (B) using the program indicated in Table S4. At the end of the analysis the column was reconditioned to the initial conditions for 15 minutes. The flow rate was 0.4 ml/min. In accordance with the absorption maximum of the UV spectrum of the three anthraquinone compounds, the following wavelengths were selected: 360 nm for the determination of aloin and 450 nm for the determination of Aloe-emodin and 1,8-dihydroxyanthraquinone (1,8-DHA). The identification of the peaks was carried out by comparing the retention time and UV spectrum of each individual compound with that of the commercially available reference standard (analytical standards Aloin A and B, Aloe-emodin, 1,8-dihydroxyanthraquinone were purchased from Extrasynthese France). The individual compounds were quantified with the external standard method by correlating the peak area with the concentration of the corresponding standard. Correlation values ranged from 0.9990 to 0.9999. The 5-point calibration line was prepared in methanol by appropriate dilution of the stock standard solution (1000 mg/l). We then proceeded with the quantitative analysis using the external standard method. The concentration of Aloin B was determined using the analytical standard of aloin A and B as a reference. All analyzes were carried out in triplicate.

MCC and MCC derived materials characterization

X-ray powder diffraction (XRPD) patterns were recorded with Cu-Kα radiation (λ = 1.54056 Å) using a Seifert x3000TT Diffractometer n the Bragg–Brentano geometry with a step size of 0.05 2θ degree in an angle range $4° \leq 2\theta \leq 50$ ° An appropriate acquisition time was selected to obtain a satisfactory signal-to-noise ratio.

ATR-FTIR spectra were recorded on a Bruker Invenio spectrophotometer equipped with a mercury-cadmium-telluride (MCT) detector with 64 scans for the background and 32 scans for the analysis of the sample. The double bond conversion was calculated by following the decrease of the double bond peak centred at 1636 cm^{-1}. The peak at 1740 cm^{-1} representing the C=O bond stretching vibration was utilized as internal standard, since it is not significantly affected by the reaction.

^{13}C CP/MAS-NMR spectra were recorded on a Bruker Avance III HD at 5kHz rotation, contact time: 2ms, delay: 3, line broadening: 10 Hz. Chemical shifts (δ) are given in ppm.

Thermo-gravimetric coupled infrared absorption analyses (TGA-IR) were carried out in a Thermo-gravimetric Analyzer NETZSCH TG 209 F1 coupled by a transfer line heated at 230 °C with an Infrared spectrometer Bruker TENSOR II equipped with an IR gas cell heated at 200 °C. The tests were performed heating from 30°C to 800°C with a rate of 20 °K min-1 about 3 mg sample in alumina pans, under nitrogen flux of 40 ml min-1. Before the test three vacuum cycle were performed to purge from air and remove solvent impurities on the surface of the materials. Experimental weight error is between ±1%. The FTIR analysis was collected in the absorbance mode in the range 650-4400 cm^{-1}.

The morphological characterization of the cellulosic materials was performed by using a FESEM Zeiss Supra 40 (Oberkochen, Germany). Before the analysis, the samples were covered with a 7 nm thick film of Platinum.

Rheological measurements were performed on the photocurable formulations using a Physica MCR 302, Anton Paar rheometer in parallel plate mode. For the photorheological tests, the gap between the plates was fixed at 0.2 mm, the instrument was equipped with a quartz bottom plate, on which the formulation was placed. A UV-light source (Hamamatsu LC8 lamp, Hamamatsu Photonics) at light intensity of 30 $mWcm^{-2}$ was placed under the quartz plate and switched on after 60 s, to allow the system to stabilize before the onset of polymerization. Time sweep measurements were performed during irradiation at a constant frequency of 1 Hz. According to preliminary amplitude sweep tests, the experiments were performed within the linear viscoelastic region (strain amplitude γ of 1%).

The insoluble fraction was evaluated to quantify the covalently crosslinked fraction of the photopolymerized or 3D printed materials. Flat samples were held in an ultra-fine metal net, weighted and immersed for 24 h at room temperature in chloroform, to remove un-crosslinked polymers (the soluble fraction). For GelMA samples water was used as solvent. Then, the samples were taken out from the bath and dried in an oven (80 °C, 6 h). The gel content (GC) was calculated gravimetrically as the ratio of the weight after and before extraction. The measurements were repeated three times and the results averaged.

Dynamic mechanical thermal analyses (DMTAs) were performed on thin specimens using a Tritec 2000 DMA (Triton Technology Ltd). The measurements were conducted in a temperature range between -50° C and 30° C (heating rate 3 °C min^{-1}), with a frequency of 1 Hz, and a displacement of 20 μm.

Results

Aloe Vera peels waste was recovered from the processing plant in September 2022; firstly, the freeze-dried and ball milled biomass was analyzed performing the ash quantification and following the Van Soest method. These characterizations allow to define the composition of the original material: ash

content witnesses the amount mineral preserved in the sample Aloe Vera powder gave an ash content of 21.95%, resulting in good agreement with data reported in literature.[20] Subsequently, quantification analyses were performed to determine the amount of insoluble fibers for Aloe Vera. The NDF, ADF and ADL measured values are reported in Table S5, these data allowed to evaluate the weight percentage of cellulose, hemi-cellulose and lignin which are reported in Table 1.

During the first step of the biomass treatment, Aloe powders were submitted to extraction using ethanol to remove the lipidic fraction, chlorophylls and the majority of anthraquinone species (AQs), which were then determined by HPLC analysis (Table 1). Part of these components can be of interest for different applications considering their antimicrobial or optical properties and will be exploited in further studies. [21,22]

Table 1. Summary of the evaluated components of Aloe Vera waste powder. Columns 1 and 2: insoluble fractions; Columns 3 and 4:Anthraquinones HPLC analysis of Aloe Vera EtOH extracts.

Measured insoluble components	Wt %	Extracted Anthraquinones	mg/kg ± SD
Lignin	10.65	Aloin A	160 ± 2
Cellulose	8.56	Aloin B	n.d.
Hemicellulose	4.61	Aloe emodin	411 ± 21
Ash (inorganic fraction)	21.95	1,8-DHA	105 ± 5

After the characterization of the original material, the cellulose extraction process was developed and the final powder obtained was first characterized by XRD, comparing its pattern with the ones from commercial MCC and with the one from the untreated waste i.e Aloe Peel powder (Figure 1a). As expected, the data show that Aloe Vera presents a similar pattern to commercial MCC, with crystallinity is of type I, and a high width at half height, suggesting that the isolated material possesses nanocrystalline domains. [23] The (200) diffraction peak around 22.5° observed in all the samples is due to the presence of the typical crystalline lattice of native cellulose Iβ, i.e. the monoclinic lattice, while the region between the cellulose Iβ (200) diffraction peak and the 1-10 peak is assumed to have very little crystalline contribution and is approximated as comprising of only an amorphous contribution. From the relative intensities of the crystalline peaks with respect to the amorphous contribution, considered at the minimum between the peaks of the X-ray diffraction spectrum, it is possible to estimate the crystallinity index (CI) of the sample, which are 90, 63, 52% for commercial cellulose, cellulose from Aloe Vera and Aloe Vera peel powder before extraction, respectively. [23,24] In this case, observing the spectrum of untreated peel of Aloe Vera, the sample shows a very low CI.

ATR-FTIR analyses also highlighted a good overlap between the spectra of commercial cellulose and the samples obtained from Aloe waste after drying (Figure 1d). Indeed, all the samples show overlap in the two main uptake regions. The first at high wave numbers (2800-3500 cm^{-1}), associated with OH

stretching, and the second at low wave numbers (500-1700 cm^{-1}) respectively, with the minimal presence of the typical peaks of hemicellulose and lignin confirming the goodness of the extraction method used.[25] In detail, the peaks at 1431, 1372, 1322, 1163, 1059 and 896 cm^{-1} are typical of the cellulose structure; e.g. the absorption band at 1163 cm^{-1} has been attributed to C-O-C stretching and the peak at 896 cm^{-1} is associated in the literature with the CH vibration of cellulose (anomeric vibration, specific for glucosides).[26]

According to various studies, the presence of a peak at 1635 cm^{-1} can be due to the bending of the –OH groups of residual absorbed water;[27–29] in the present case, it is possible to observe the presence of the above mentioned peak presenting a shoulder at 1554 cm^{-1} that can be associated to the residual presence of ligning.While the peak at 1730 cm^{-1} can be associated to residual hemicellulose fraction. [26-29] SEM images taken at different magnitudes were also performed to observe the morphology variation of the extracted cellulose from Aloe biomass and value the efficiency of the multistep MCC preparation (see Supporting Information). Figures 1b and 1c show appreciable changes in the morphology and organization of the fibers in Aloe Vera samples due to the hydrolysis and bleaching process.

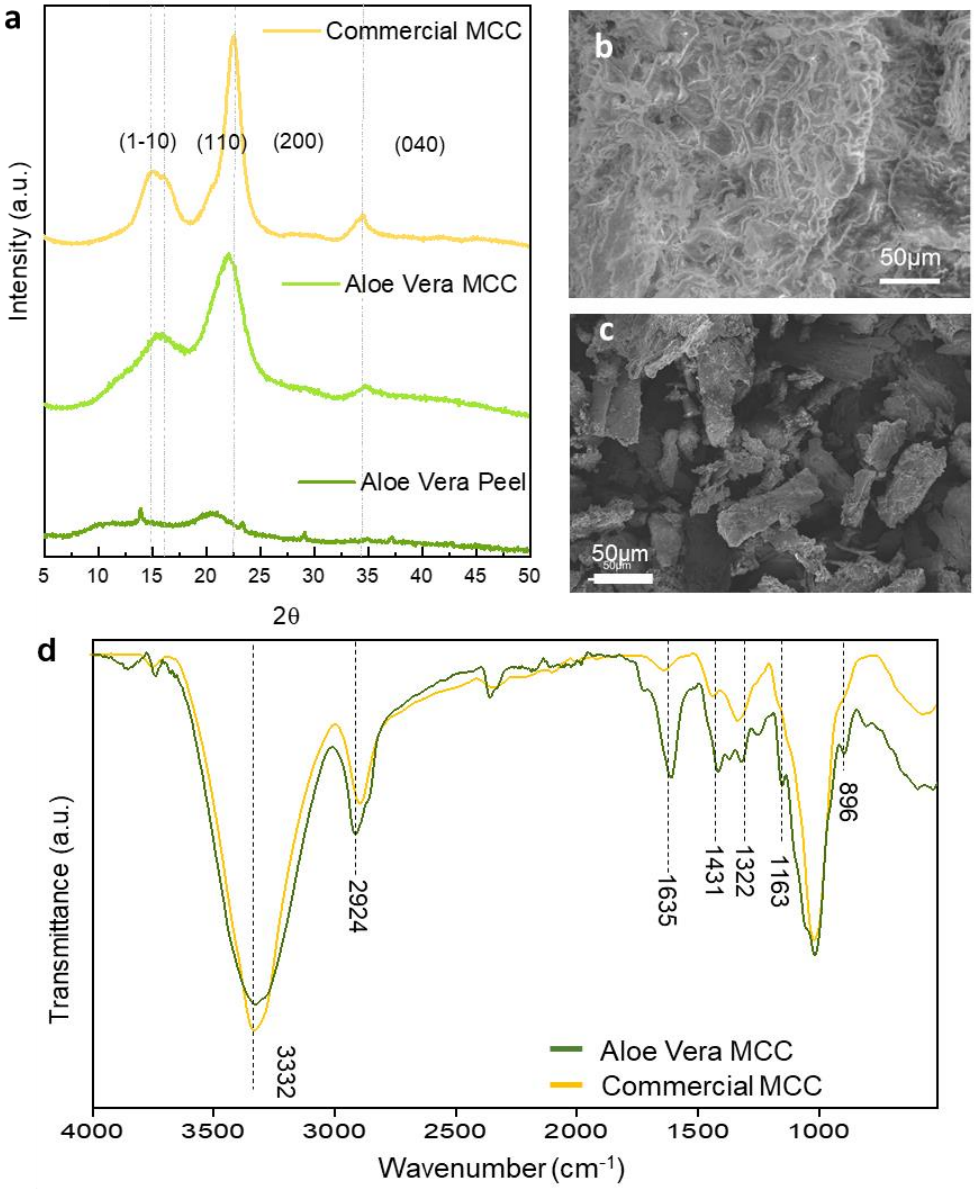
a
Commercial MCC
(1-10)
(110)
(200)
(040)
Intensity (a.u.)
Aloe Vera MCC
Aloe Vera Peel
5
10
15
20
25
30
35
40
45
50
2θ
b
50μm
c
50μm
d
Transmittance (a.u.)
3332
2924
1635
1431
1322
1163
896
Aloe Vera MCC
Commercial MCC
4000
3500
3000
2500
2000
1500
1000
Wavenumber (cm-1)

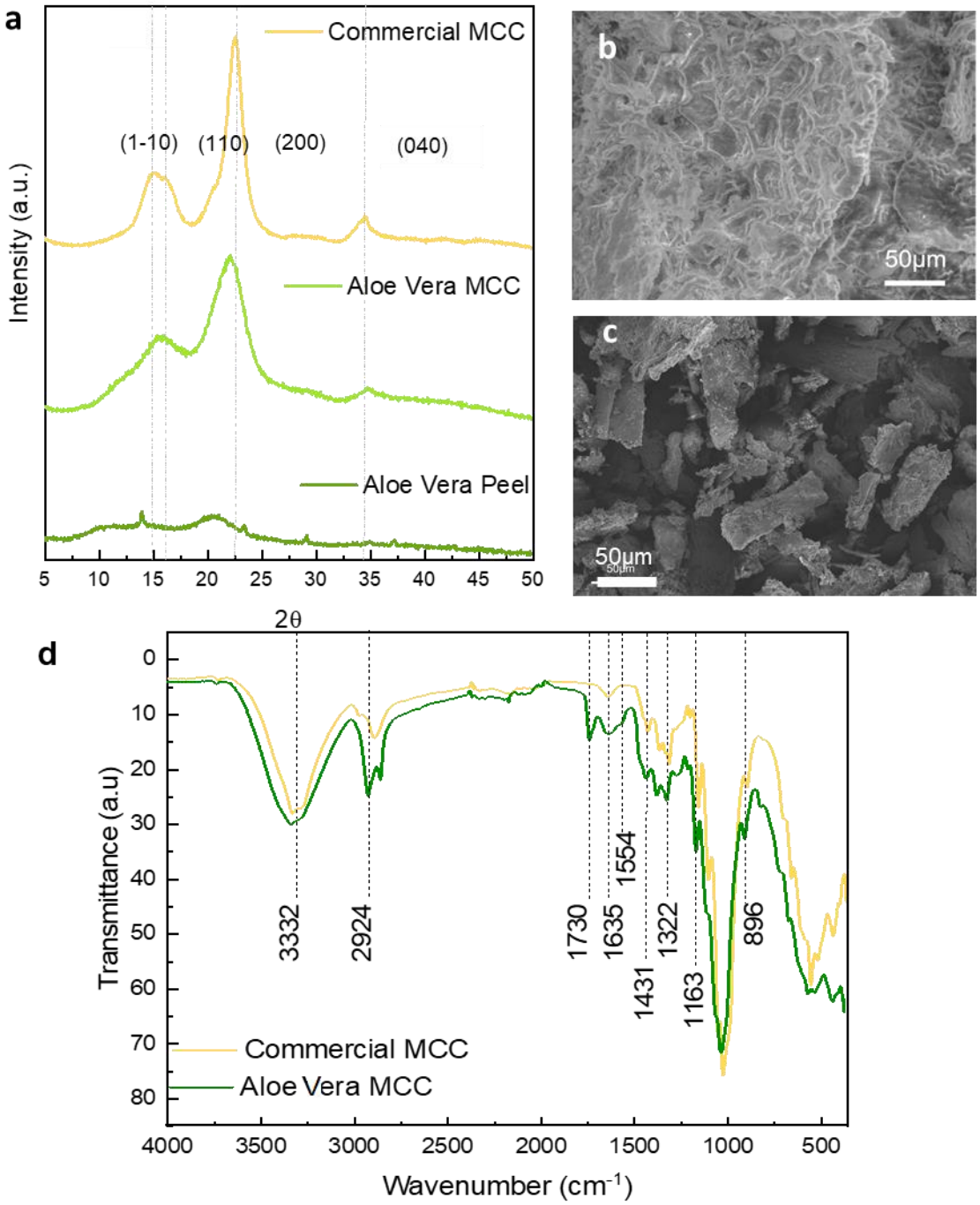

Figure 1. a) X-ray diffraction analysis Aloe Vera peel powder, commercial cellulose, and cellulose from Aloe Vera; b) SEM image of Aloe Vera peel; c) SEM image of Aloe Vera MCC (50 µm); d) ATR-Infrared Spectrum collected on the extracted MCC and compared to commercial MCC

In the images is possible to appreciate the removal of the cementing material which is normally arranged around the cellulosic fibers, mainly composed of hemicellulose and lignin. Cellulose fibers appear polydisperse and disorganized, showing the complete loss of the original alveolar structure (Figure 3e).

Once characterized the extracted cellulose, we decided to modify it by introducing a series of functional groups showing the potentiality of MCC from waste as platform for developing new materials. A sequence of functional groups were selected: a) methacrylic anhydride, b) phthalic anhydride, c) phthaloyl chloride followed by allylamine d) 4-bromo-benzoyl chloride. As an example, MCC functionalized with methacrylic anhydride could be subsequently exploited in radical polymerization, while the presence of a Br-bearing molecule or an allyl group could be envisaged for further functionalization by ATRP or click chemistry for the surface modification of the material, alternatively, the presence of a carboxylic group can be exploited for amide formation. [30–33] The different reactions are represented in Figure 2.

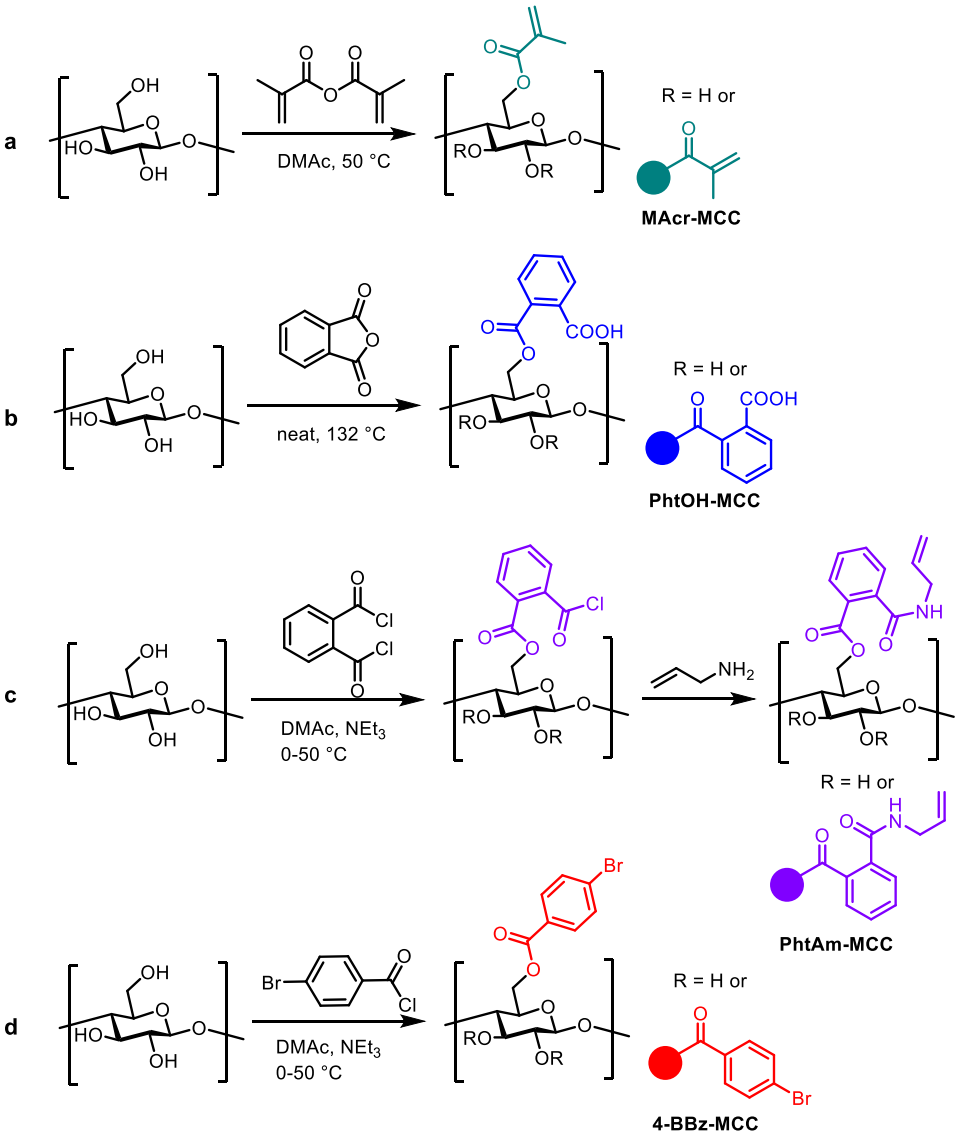

Figure 2. Synthesis of cellulose esters: (a) MAcr-MCC; (b) PhtOH-MCC; (c) PhtAm-MCC; (d) 4-BBz-MCC) from Aloe Vera MCC.

The functionalized MCC derivatives were investigated via ^{13}C CP/MAS to quantify their degree of substitution (DS). Solid-state NMR analyses of MAcr-MCC showed comparable spectra with those previously reported in the literature. By referencing the signal at 19.5 ppm, attributed to the methyl group of the methacrylic units[34] (Figure S9) and correlating its area with that of the characteristic signals of MCC we were able to quantify the DS of MAcr-MCC as 6.1%. This value was further confirmed by Br_2 titration (6.2%).[35] Similarly, CP/MAS analysis of other MCC derivatives enabled determination of their degree of substitution. Specifically, PhtAm-MCC exhibited a DS of 3.1% (Figure S8), BBz-MCC showed a DS of 2.8% (Figure S10), and PhtOH-MCC had a DS of 1.6% (Figure S11). The latter data was also verified through acid-base back-titration (1.65%), utilizing the methodology previously established by Neale and Stringfellow.[36] ATR analyses were also performed on the same samples, confirming the functionalization of the Aloe MCC as reported in the SI.

Thermogravimetric analyses are in good agreement with NMR and IR experiments, confirming the presence of functionalization on cellulose. Besides the final residue, which can belong to various factor including the type of functionalizing molecule and extent of functionalization, noteworthy the functionalized MCCs presented different degradations steps, evidenced by the presence of difference peaks in DTG. MAcr-MCC and PhtAm-MCC show a main degradation moment around 360°C, similar to the starting material; however, methacrylate has a second loss, that overlaps with the first degradation observable by a change in the slope of the thermogravimetric curve near 400°C (Figures 3b and 3d). For the phthalate derivative PhtOH-MCC or the 4-bromo benzoyl (4-BBz -MCC) derivative (Figures 3c and 4e) instead, we observe that the degradation of the material begins before the pure cellulose and we distinctly observe two stages of the decomposition: for the phthalate derivative we have two steps with two maximum peaks of degradation respectively at about 220 °C, with a first loss close to 80% of mass, and 350 °C with a second loss of about 15% of the total mass. For 4-BBz-MCC we observe a maximum of degradation at the first step at about 290 °C and a second loss at around 360 °C with two almost symmetrical mass losses of about 40% of total mass for both steps. On the other hand, from the IR extrapolated at the maximum of DTGs curves, it was possible to obtain information about the volatilized degradation by-products and, in turns, about the materials. First, as expected, all the spectra show the development of CO_2, CO, and H_2O due to polymer degradation. However, the comparison of MCC and MAcr-MCC spectra shows important differences in the fingerprint bands, where symmetric stretching of C-O-C acrylates is observed at 1150 cm^{-1} only in MAcr-MCC specimens confirming the presence of unsaturated bonds. Significant losses were attributed to specific functional groups like in the case of 4-BBz-MCC (Figure 3e'), where the IR analysis during the degradation step showed the rise of a series of peaks helpful for the identification of the carboxylic moiety, evidenced by the C=O and

O-H carboxylic stretching, respectively at 1750 cm^{-1} and 3600 cm^{-1}. In phthalic anhydride degradation, it is evident at 220 °C the sublimation of phthalic anhydride, confirmed by comparison with the spectrum of phthalic anhydride present in the NIST databases. In the second observed mass loss at 352.7 °C, other peaks related to reacted phthalic anhydride degradation are observed: the carboxyl stretching at 1743 and 3600 cm-^{1}, and the presence of both the C=O ester stretching peak at 1800 cm^{-1}.

Table 2. Percentage mass losses at the respective degradation stages and the percentage residual mass detected.

Entry [b]	1st degradation (220°C)	2nd degradation (360 °C)	Residual mass (795 °C)
MCC	-	84.51%	7.66%
MAcr-MCC	-	89.52%	5.26%
PhtOH-MCC	77.63%	14.79%	3.18%
PhtAm-MCC	-	79.80%	12.82%
4-BBz-MCC	45.41%	46.45%	3.82%

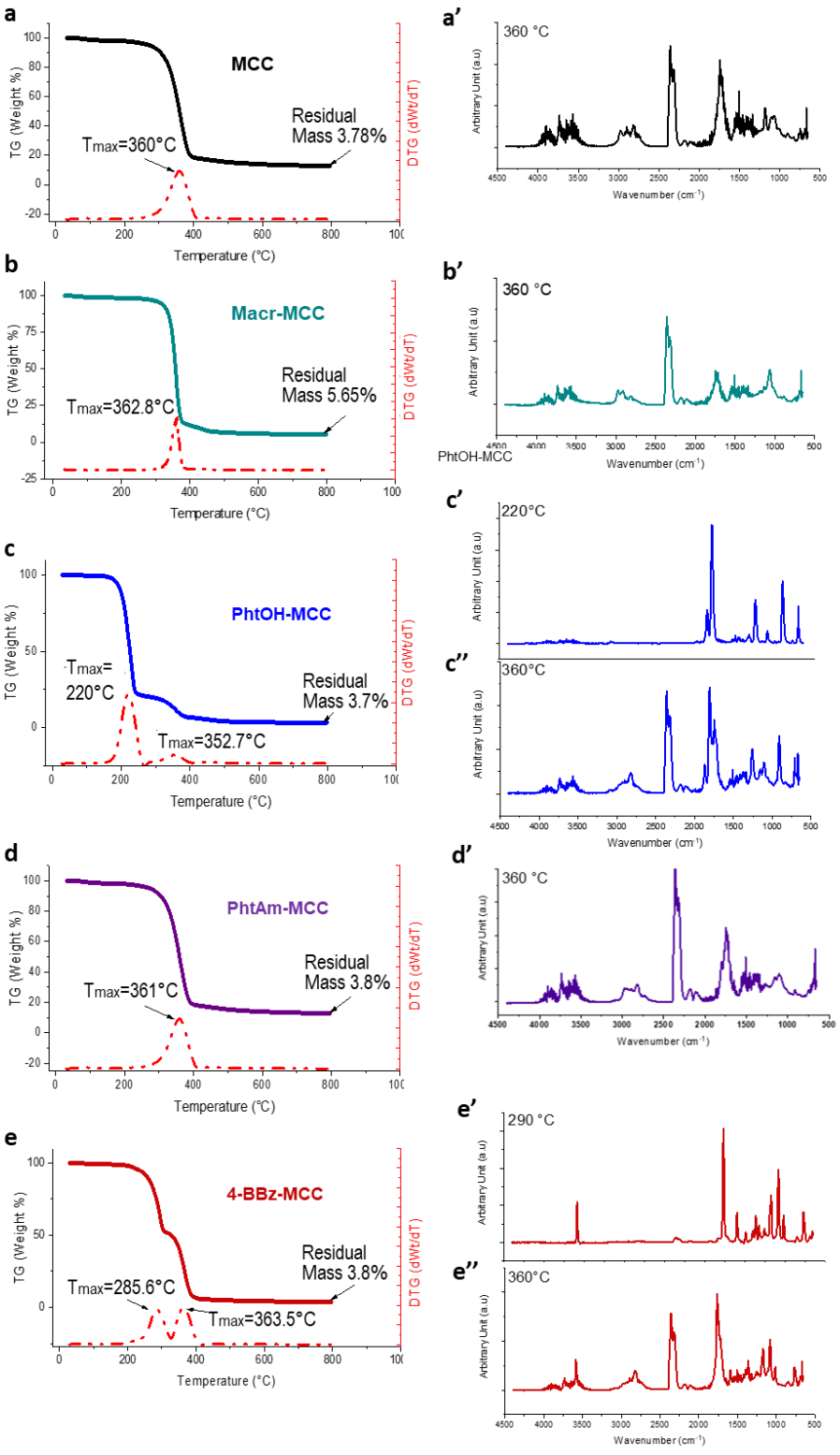

Figure 3. (a) TGA-IR analyses of extracted Aloe Vera MCC after bleaching and hydrolysis; (black); (b) MAcr-MCC (cyano); (c) PhtOH-MCC (blue); (d) BBz-MCC (purple) and (e) PhtAm-MCC (red).

Regarding the two steps functionalization of MCC to afford PhtAm-MCC, the IR spectrum extracted at 360° C shows the presence of a peak at 2945 cm^{-1} (S7a) which was attributed to the allylic C-H stretching, suggesting that the allylamine fragment is already connected to MCC. Moreover, IRs recorded during the second degradation step are characterized by a peak at 1145 cm^{-1}, (S7b) that can be related with the amide N-C=O rocking. SEM images of the functionalized MCC particles were also collected and are reported in the Supporting Information file, Figures S12.

With these information in hands, MAcr-MCC was chosen to be used as filler and crosslinker in different photocurable formulations, aiming to produce bio-based composites which can be also processed by light induced vat 3Dprinting.

First, MAcr-MCC was added as filler in methacrylated gelatine (GelMA) hydrogels, synthesizing a fully natural-based material. Gelatine is a natural polymer, used for development of hydrogels, usually for environmental or tissue engineering applications. [18,34] Different amounts of MAcr-MCC (5, 10 wt% with respect to the total solution weight) were added to GelMA water solutions (15wt% of GelMA), in the presence of a water-soluble photoinitiator. The evaluation of the viscosity of the formulations (named G-MAcr-MCC -5 or 10) showed, as expected, a remarkable increase of viscosity in the presence of the cellulose particles (Figure 4a). The addition of not functionalized MCC was also tested as a comparison (samples G-MCC 5 or 10) and showed a higher increase of the viscosity with the same concentrations; this can be explained considering that in MAcr-MCC part of the OH groups present on the cellulose surface were substituted with acrylic groups, reducing the formation of hydrogen bonds between the particles and the polymer in the formulation. Photorheology tests were performed to evaluate the reactivity of the formulations (Figure 4b). Compared with the formulations containing MCC, MAcr-MCC increases the reactivity of the formulations, reducing the induction time (time needed to observe the start of the increase of the G' modulus curve). The higher G' values that can be observed before the polymerization are related to a more viscous formulation. At last, amplitude sweep tests, performed on the cured samples, (Figure 4, c) showed higher modulus and lower yield point at higher MAcr-MCC concentrations, confirming the reinforcing effect of the cellulose microparticles. The tuning of the viscosity and reactivity of the formulations can enlarge the application possibilities for the material, also enabling its 3D printing. Indeed, the characteristics shown by the G-MAcr-MCC formulations, and consequently were used as inks for vat 3D printing. The G-MAcr-MCC5 formulation was printed by DLP technique, since it showed a good compromise between reactivity and initial viscosity. DLP allows the fast production of 3D constructs with complex geometry, but it requires low initial viscosity, good reactivity and sufficient mechanical stability of the printed polymers to assure the bottom-up building of the object (see Scheme in the SI. Figure S6).[35] The preliminary printing test showed that the formulation can be printed and patterned objects can be built (Figure 4d and e); furthermore, the comparison with a formulation containing MCC revealed the better mechanical stability given by the multiacrylated filler which acted also as chemical crosslinker for the hydrogel. In

fact, while the MAcr-MCC based formulation gave homogeneously printed samples, the ink based on neat MCC did not allow the complete printing of the structures (Figure 4f). The increase of the crosslinking density of the MAcr-MCC sample was also evidenced by the swelling tests in water, evidencing a great reduction of the swelling induced by the presence of the cellulose (Figure 4g).

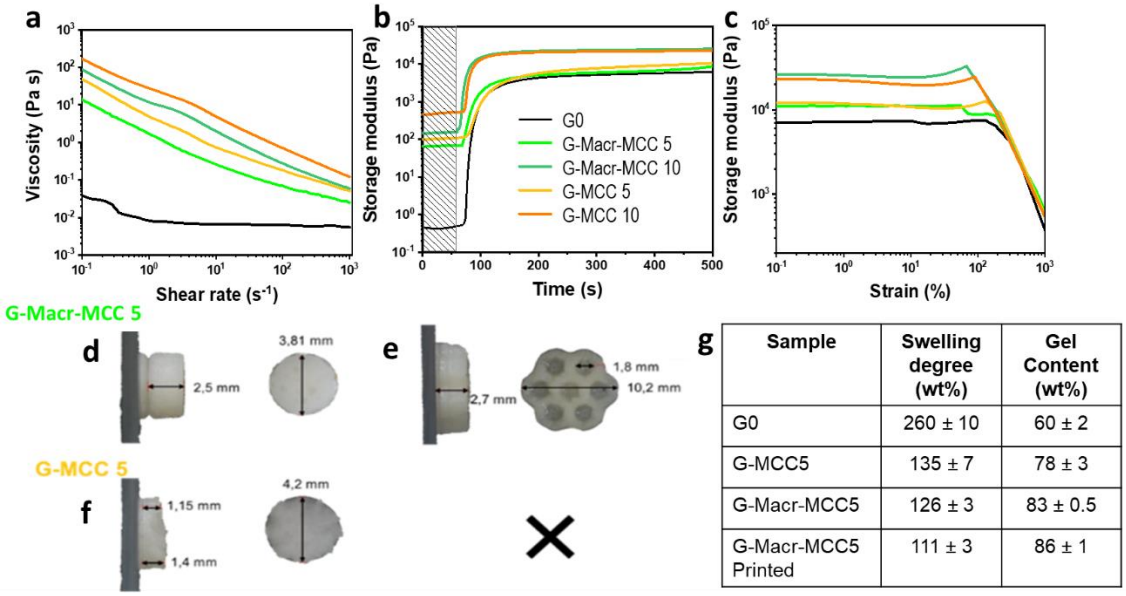

Sample	Swelling degree (wt%)	Gel Content (wt%)
G0	260 ± 10	60 ± 2
G-MCC5	135 ± 7	78 ± 3
G-Macr-MCC5	126 ± 3	83 ± 0.5
G-Macr-MCC5 Printed	111 ± 3	86 ± 1

Figure 4. (a) Viscosity measurements performed on GelMa (black), GelMa MAcr-MCC 5% (light green), GelMa MAcr-MCC 10% (dark green), GelMa MCC 5% (yellow) GelMA MCC 10% (orange)(b) photorheology tests, (c) amplitude sweep measurements) (d,e) different structures produced by DLP printing using the formulation based on GelMa and MAcr-MCC 5wt% (f) tentative of DLP printing with the formulation based on GelMa and neat MCC 5wt%, it was not possible to buid the honeycomb structure (g) swelling ability and gel content of the different samples.

The swelling trend suggests that also neat MCC can act as physical crosslinker, nevertheless the reduction of the swelling ability was more evident when using acrylate fillers. Also the evaluation of the amount of insoluble fraction in the samples (gel content) led to similar conclusions: while from GelMA itself a large fraction of non-crosslinked components can be extracted, the use of MAcr-MCC increases the crosslinking and the gel content in the samples. The use of neat MCC alos reduces the amount of extractables (i.e., non-crosslinked components). Beside the development of fully-biobased hydrogels, acrylate-functionalized cellulose was also tested as filler for synthetic commercial photocurable monomers; polyethylene glycol diacrylate (PEGDA) was chosen as bifunctional oligomer largely used for photopolymerization and DLP printing.[35] As observed in the case of GelMA, the addition of the filler increases the viscosity of the liquid formulation (Figure 5a), even if in this case the use of 20wt% of MAcr-MCC still induces a limited variation, while higher amounts (i.e 33wt%) cause

a drastic increase of the viscosity, giving to the formulation the consistency of a paste and making it unsuitable for vat 3D printing. Nevertheless, such pastes can be considered for other 3D printing technologies, such DIW (Table S6). Again, the formulations were compared with MCC-based ones, obtaining even in this case a higher increase of viscosity.

According to the photorheology tests, the addition of MAcr-MCC does not limit the reactivity up to a content of 33 wt% (Figure 5b), with the formation of fully crosslinked network witnessed by the measurement of the insoluble fraction content, always higher than 98%. Also the evaluation of the acrylate double bond conversion confirms that the presence of the filler does not hinder the crosslinking of the monomer (Table S6, Figure S15). Furthermore, all these formulations can be photocured forming homogenous films (Figure S14). The obtained films were tested by DMTA analysis showing an increase of the E' value (conservative modulus) at room temperature with the increase of the amount of Mcr-MCC used. Thus, the formulation containing 20wt% of MAcr-MCC was used in VAT 3D printing. The printing tests showed the possibility to produce precise objects with complex geometries (Figure 5c) presenting good fidelity to the CAD digital model, as evidenced by the comparison of the 3D scan of the printed object with the original CAD file reported in Figure 5d; this investigation indicates the geometrical deviation from the reference model, where the red zones represent the "material-excess" and the green ones correspond to areas with good fidelity. Noteworthy, such good resolution was obtained without the addition of any dye, which usually are used to this scope. [35]

The formulations prepared and successfully printed by DLP technique demonstrated that MCC extracted form Aloe waste can be used even up to 20wt% as bio-based component for 3D printable formulations.

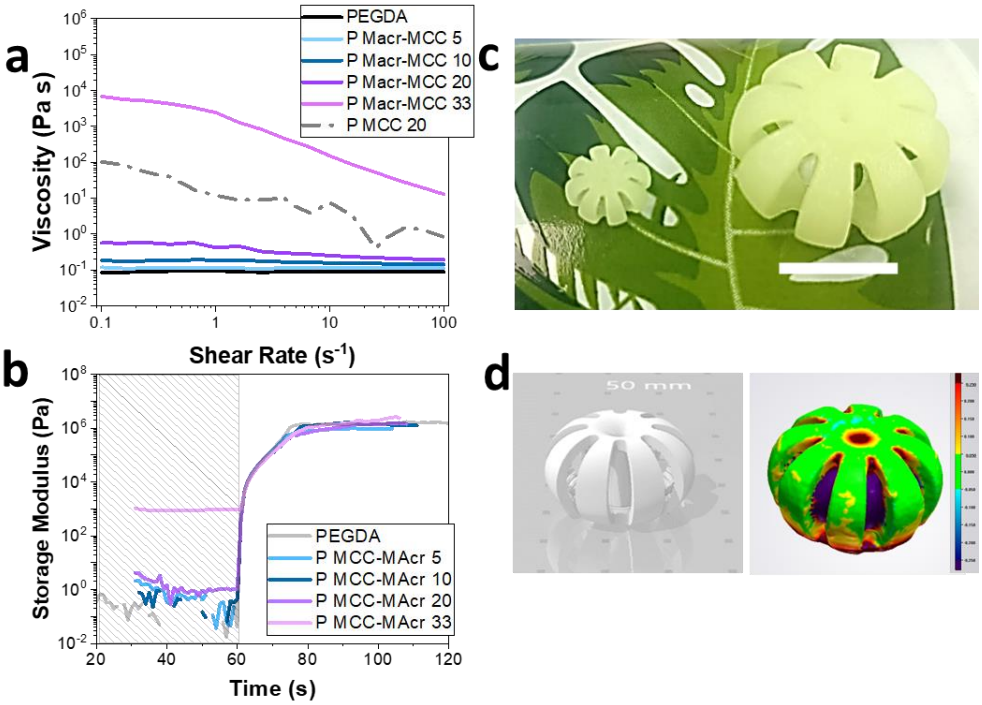

Figure 5. (a) Viscosity measurements (b) Photorheology tests (c) 3D objects produced by DLP printing using the PEGDA formulation containing 20 wt% of MAcr-MCC, scale bar 1 cm (d) CAD design (left) and color map of the comparison between the 3D scan of the printed object and the original CAD file. Green area represents a maximum deviation from the original file of 50µm.

Conclusion

It has been shown that local agrifood waste can be valorized and turned into an active component for chemical reactions such as photopolymerization. Indeed, Aloe waste collected from local Sardinian cultivation was here employed to prepare microcrystalline cellulose. The cellulose extraction and the purification process were performed using mild reaction conditions. After the characterization of the extracted materials by ATR and XRD, MCC was functionalized with different reactive groups showing the possibility to convert these bioderived particles into functional elements; as a proof of concept, methacrylated cellulose was used as reactive filler and crosslinker in 3D printable formulations, showing its potential for different applications. Noteworthy, it has been evaluated that 1 kg of waste of Aloe Vera peels contains about 8.5wt% of cellulose (85g), which can be used to produce more than 400 g of photocurable formulation suitable for 3D DLP printing, indicating that from such waste material it is possible to generate materials whit added value, especially considering that resins for DLP costs about 50 USD per Kg. Beside this proposed application, cellulose derivatives can find their utility in several fields as well as the different components separated from the waste e.g. lignin or antraquinones.

Acknowledgements

VIVA3D- Ministero dell'Ambiente e della Tutela del Territorio e del Mare project is gratefully acknowledged for research fundings. FSC 2020-Piano Stralcio (Fondo per lo Sviluppo e la Coesione - DOT1304455) is gratefully acknowledged for financing Maria Chiara Cabua's PhD grant. The authors acknowledge the University Research Services Centre (CeSAR)-UniCA for technical support. Francesco Secci and M. Chiara Cabua acknowledge Sa Corona Arrubia Consortium-Collinas (Italy) for all the technical support during the project development.

Associated Content

Supporting Information available. [Additional experimental details; FTIR analysis of functionalized MCC derivatives, NMR analysis (^{13}C CP/MAS measurements), degree of substitution (DS); SEM images of MCC-derivatives and DLP printing schemes of functionalized cellulose derivatives are provided]

References:

1. Gunjan; Chopra, L.; Manikanika. Extraction of cellulose from agro waste – A short review. *Mater Today Proc*. 2023, 92, 233-239.

2. Maji, S; Dwivedi, D. H.; Singh, N.; Kishor, S.; Gond, M. *Agricultural Waste: Its Impact on Environment and Management Approaches*. **2020**, 329-351.

3. Duque-Acevedo, M.; Belmonte-Ureña, L. J.; Cortés-García, F. J.; Camacho-Ferre, F. Agricultural waste: Review of the evolution, approaches and perspectives on alternative uses. *Glob. Ecol. Conserv*. **2020**, 22:e00902.

4. Zhang, Y.; Ni, S.; Wu, R.; Fu, Y.; Qui, M.; Willför, S.; Xu, C. Green fractionation approaches for isolation of biopolymers and the critical technical challenges. *Ind. Crops. Prod*. **2022**, *177*, 114451-114460.

5. Freixo, R.; Casanova, F.; Ribeiro, A. B.; Pereira, C. F.; Costa, E. M.; Pintado, M. E.; Ramos, O. L. Extraction methods and characterization of cellulose fractions from a sugarcane by-product for potential industry applications. *Ind Crops Prod*. **2023**, *197*, 116615-116625.

6. Kaur, S.; Bains, K. Aloe Barbadensis Miller (Aloe Vera). Int. J. *Vitamin Nutrition Res*. **2023**, doi:10.1024/0300-9831/a000797

7. Boudreau, M. D.; Beland, F. A. An Evaluation of the Biological and Toxicological Properties of Aloe Barbadensis (Miller), Aloe Vera. J. *Environm. Sci. Health Part C.* **2006**, *24*, 103-154.

8. Gao, Y.; Kuok, K. I.; Jin, Y.; Wang, R. Biomedical applications of Aloe vera. *Crit. Rev. Food. Sci. Nutr.* **2019**, *59*, 244-256.

9. Eshun, K, He, Q. Aloe Vera: A Valuable Ingredient for the Food, Pharmaceutical and Cosmetic Industries-A Review. *Crit Rev Food Sci Nutr*. **2004**, *44*, 91-96.

10. Singh, A.; Verma, K.; Kumar, D.; Nilofer, Nikil, B. L.; Kumar A.; Chaudhary, A.; Kaur, P.; Singh, K. P.; Singh, A. K.; Kumar, R.; Anandakumar, T. M.; Singh, S. Optimized irrigation regime and

planting technique improve yields and economics in aloe vera [Aloe barbadensis (Miller)]. *Ind. Crops Prod*. **2021**, *167*, 113539-113547.

11. Giannakoudakis, D. A.; Hosseini-Bandegharaei, A.; Tsafrakidou, P.; Triantafyllidis, K. S.; Kornaros, M.; Anastopoulos, I. Aloe vera waste biomass-based adsorbents for the removal of aquatic pollutants: A review. *J. Environ. Manage*, **2018**, *227*, 354-364.

12. Srivastava, D.; Sharma, D.; Ali, N. Biomethanation of Aloe Vera Waste for Energy Production. *Lect. Notes Mechan. Eng.* **2021**, 139-147.

13. Semerel, J.; Dehaen, J. N. W.; Fardim, P. Valorization of Aloe barbadensis Miller. (Aloe vera) Processing Waste. *J. Renew. Mater*. **2022**, *11*, 1031-1061.

14. Luo, K.; Wang, Y.; Xiao, H.; Song, G.; Cheng, Q.; Fan, G. Preparation of convertible cellulose from rice straw using combined organosolv fractionation and alkaline bleaching. *IOP Conf. Ser*. **2019**, 237, 52053-52059.

15. Marsano, E.; De Paz, L.; Tambuscio, E.; Bianchi, E. Cellulose methacrylate: synthesis and liquid crystalline behaviour of solutions and gels. *Polym.* **1998**, *39*, 4289-4294.

16. Malm, C. J.; Mench, J. W.; Kendall, D. L.; Hiatt, G. D. Aliphatic acid esters of cellulose. Preparation by acid-chloride-pyridine procedure. *Ind. Eng. Chem.* **1951**, *43*, 684-688.

17. Peng, F.; Ren, J.-L.; Sun, X.-F.; Xu, F.; Sun, R.-S.; Peng, B.; Sun, J.-X. Rapid phthaloylation and succinylation of hemicelluloses by microwave irradiation. *e-Polymers*. **2008**, *108*, 1231-1242.

18. Noè, C.; Zanon, M.; Arencibia, A.; Lòpez-Munoz, M.-J.; Fernández de Paz, N.; Calza, P.; Sangermano, M. UV-Cured Chitosan and Gelatin Hydrogels for the Removal of As(V) and Pb(II) from Water. *Polymers*, **2022**, *14*, 1268-1287.

19. Van Soest, P. J.; Robertson, J. B.; Lewis, B.A.; Methods for Dietary Fiber, Neutral Detergent Fiber, and Nonstarch Polysaccharides in Relation to Animal Nutrition. *J. Dairy Sci.* **1991**, *74*, 3583-3597.

20. Haque MZ, Islam MB, Jalil MA, Shafique MZ. Proximate Analysis of Aloe Vara Leaves. *IOSR J. Appl. Chem.* **2014**, *7*, 36-40.

21. Qun, T.; Zhou, T.; Hao, J.; Wang, C.; Zhang, K.; Xu, J.; Wang, X. ; Zhou, W. Antibacterial activities of anthraquinones: structure–activity relationships and action mechanisms. *RSC Med. Chem.* **2023**, *14*, 1446-1471.

22. Yan, X.; Huang, N. Effects of Three Different Types of Aloin on Optical, Mechanical, and Antibacterial Properties of Waterborne Coating on Tilia europaea Surface. *Coatings*. **2021**, *11*, 1537-1552.

23. Park, S.; Baker, J.O.; Himmel, M.E.; Parilla, P.A.; Johnson, D.K. Cellulose Crystallinity Index: Measurement Techniques and Their Impact on Interpreting Cellulase Performance. *Biotechnol. Biofuels*, **2010**, *3*, 1-10.

24. Segal, L.; Creely, J.J.; Martin, A.E.; Conrad, C.M.; Opportunity for New Developments in All Phases of Textile Manufacturing. ' Literature Cited An Empirical Method for Estimating the Degree of Crystallinity of Native Cellulose Using the X-Ray Diffractometer. *Textile Res. J.* **1959**, *29*, 786-794.

25. Abidi, N.; Cabrales, L.; Haigler, C.H. Changes in the cell wall and cellulose content of developing cotton fibers investigated by FTIR spectroscopy. *Carbohydr. Polym.* **2014**, *100*, 9-16.

26. Ibrahim, M.M.; El-Zawawy, W.K.; Jüttke, Y., Koschella, A.; Heinze, T. Cellulose and microcrystalline cellulose from rice straw and banana plant waste: Preparation and characterization. *Cellulose*. **2013**, *20*, 2403-2416.

27. Javier-Astete, R.; Jimenez-Davalos, J.; Zolla, G. Determination of hemicellulose, cellulose, holocellulose and lignin content using FTIR in Calycophyllum spruceanum (Benth.) K. Schum. And Guazuma crinita Lam. *PLoS One*. **2021**, *16*, e0256559.

28. Zhou, C.; Jiang, W.; Cheng, Q.; Via, B.K. Multivariate calibration and model integrity for wood chemistry using fourier transform infrared spectroscopy. *J. Anal. Methods Chem.* **2015**, 1-9.

29. Zhang, f.D.; Xu, C.H.; Li, M.Y.; Chen, X.D.; Zhou, Q.; Huang, A.M. Identification of Dalbergia cochinchinensis (CITES Appendix II) from other three Dalbergia species using FT-IR and 2D correlation IR spectroscopy. *Wood Sci. Technol*. **2016**, *50*, 693-704.

30. Cafiso, D.; Septevani, A.A.; Noè, C.; Schilleri, T.; Pirri, C. F.; Roppolo, I. Chiappone, A. 3D printing of fully cellulose-based hydrogels by digital light processing. *Sus. Mater. Technol*. **2022**, *32*, e00444.

31. Lindqvist, J.; Nyström, D.; Östmark, Per, A.; Carlmark, A.; Johanson, M.; Hult, A.; Malmstrom, E. Intelligent Dual-responsive cellulose surfaces via surface-initiated ATRP. *Biomacromol*. **2008**, *9*, 2139-2145.

32. Liang, H.; Yin, D.; Shi, L.; Liu, Y.; Hu, X.; Zhu, N.; Guo, K. Surface modification of cellulose via photo-induced click reaction. *Carbohydr. Polym.* **2023**, *301*, 120321-120340.

33. Pettignano, A.; Charlot, A.; Fleury, E. Solvent-Free Synthesis of Amidated Carboxymethyl Cellulose Derivatives: Effect on the Thermal Properties. *Polymers*, **2019**, *11*, 1227-1245.

34. Chen, T. ; Liu, W. Highly unsaturated MicrocrystallineCellulose and its Cross-LinkedSoybean-Oil-Based termosetComposites. *ACS Sus. Chem. Eng*. **2019**, *7*, 1796-1805.

35. Lin, M.-S. ; Chen, A.-J. ; Preparation and characterization of water soluble and crosslinkable cellulose acrylate, *Polym.* **1993**, *34*, 389-393.

36. a) Neale, S. M.; Stringfellow, W. A. The determination of the carboxylic acid group in oxycelluloses. *Trans. Faraday Soc*. **1937**, *33*, 881-889; b) Lin, S.; Y.; Dence, C.; W. Determination of Carboxylic groups, *Methods in Lignin Chemistry*, *Springler*, **1992**, 446-457.

37. Piao, Y.; You, H.; Xu, T.; Bei, H.-T.; Piwko, I. Z.; Kwan, Y. Y.; Zhao, X. Biomedical applications of gelatin methacryloyl hydrogels. *Engin. Regeneration*. **2021**, *2*, 47-56.

38. Gastaldi, M.; Cardano, F.; Zanetti, M.; Viscardi, G.; Barolo, C.; Bordiga, S.; Magdassi, S.; Fin, A.; Roppolo, I. Functional Dyes in Polymeric 3D Printing: Applications and Perspectives. *ACS Materials Lett*. **2021**, *3*, 1-17.